Effects of Multipath-Induced Angular Spread on Direction of Arrival Estimators in Array Signal Processing*

Randolph L. Moses†, Torsten Söderström, and Joakim Sorelius
Systems and Control Group
Department of Technology
Uppsala University
P.O. Box 27, S-751 03 Uppsala, Sweden

Abstract

We consider the effects of multipath on three array signal processing algorithms for direction of arrival (DOA) estimation. We adopt a model in which the source signals impinge on an array of sensors over a spread of angles. Such a scenario arises in mobile telecommunications, where the angular spread is caused by multipath from a large number of scatterers local to each source. We analyze the effect of this angular spread on the DOA estimates obtained from MUSIC, ESPRIT, and weighted subspace fitting (WSF). We develop analytical expressions for the bias of the DOA estimates, and discuss variance properties, for small source spread angles. We compare the various techniques, and validate the analysis with simulation results.

I. Introduction

Over the past several years, a number of techniques have been developed for estimating the directions of arrival of multiple signals impinging on an array of sensors; these include MUSIC, ESPRIT, weighted subspace fitting (WSF), Maximum Likelihood (ML) methods, and their variants. Nearly all of these algorithms assume that the source signals arrive at discrete, distinct angles. This assumption leads to a signal subspace of low rank, and the low-rank property is exploited to arrive at estimates of the source directions of arrival (DOA). However, in many problems of interest, the signals do not arrive at a discrete angle but instead at a continuum of angles due to multipath from local scattering at the source transmitters. In the mobile telecommunication application, for example, signal spread from mobile transmitters has been reported [1, 2].

One approach to address such multipath is to model and estimate the signal source spread. In [3], a maximum likelihood algorithm is proposed to estimate the nominal arrival angle θ_0 and the angular spread σ_θ of each source. The algorithm has good statistical properties, but involves minimization of a nonlinear function, and can be computationally prohibitive for a general array configuration or for multiple source signals. Another approach is to analyze how perturbations on the signal model and/or

*This work has been supported by grants from the Swedish Institute, by NUTEK under project number 93–03103, and by the U.S. Army Research Laboratory under Contract DAAL01-93-C-0095.

†On leave from Dept. of Electrical Engineering, The Ohio State University, Columbus, Ohio, USA

or noise model impact DOA estimation performance (see, *e.g.*, [4, 5, 6] and their references). Existing analyses often assume an array perturbation which preserves the low rank property of the signal subspace; in contrast, the source signal spread destroys the low rank property.

In this paper, we investigate the combined effects of finite samples and dispersive multipath on three standard DOA estimation techniques: MUSIC, ESPRIT, and WSF. We assume that each source signal arrives at a continuum of angles; the power distribution of each source is described by a mean value θ_k and variance σ_k^2. We require no parametric model of the signal distribution; thus, our analysis includes both the uniform and the Gaussian multipath models proposed in [1, 2], or other models. We assume that the angular spread variances are small, and develop a first order (in σ_k^2) analysis of the bias and variance of the DOA estimates resulting from such a signal scenario. Our analysis is in part an extension of recent work by Kangas, Stoica and Söderström, who consider a general perturbation scenario for MUSIC and ESPRIT [5, 6]; we extend these results to the signal multipath scenario of interest, and also analyze the WSF method.

II. Model and Assumptions

We assume an array of m sensors, whose sampled output at time t is a complex m-vector $\mathbf{x}(t) = [x_1(t), \ldots, x_m(t)]^T$. The n uncorrelated source signals $\{s_k(t)\}_{k=1}^n$ impinge on the array; each source arrives at the array via a large number L of independent local reflectors around the source. The received signal at the ith sensor can be expressed as:

$$x_i(t) = \sum_{k=1}^{n} \left[s_k(t) \sum_{l=1}^{L} \alpha_l(t) a_i(\theta_k + \tilde{\theta}_{kl}(t)) \right] + n_i(t), \quad i = 1, \ldots, n \tag{2.1}$$

where θ_k is the nominal DOA of $s_k(t)$, $\tilde{\theta}_{kl}(t)$ is the angular deviation of the lth ray due to local scattering, and $\alpha_l(t)$ is the random complex gain of the lth ray. The array gain at angle θ is given by $\mathbf{a}(\theta) = [a_1(\theta), a_2(\theta), \ldots, a_m(\theta)]^T$. The $n_i(t)$ term is the noise component, and we assume the noise vector $\mathbf{n}(t) = [n_1(t), \ldots, n_m(t)]^T$ is a zero mean, circularly complex random vector with $E\{\mathbf{n}(t)\mathbf{n}^*(s)\} = \lambda^2 \mathbf{I}_m \delta_{t,s}$ and $E\{\mathbf{n}(t)\mathbf{n}^T(s)\} = 0$. We assume L is large in equation (2.1), and that the complex ray gains are zero mean and uncorrelated.

If the source signals have no angular spread (*i.e.*, if $\sigma_k^2 \equiv 0$), then the array covariance matrix $\mathbf{R} \stackrel{\triangle}{=} E\{\mathbf{x}(t)\mathbf{x}^*(t)\}$ is given by the standard "nominal" expression:

$$\mathbf{R}_0 = \mathbf{A}(\boldsymbol{\theta}_0)\mathbf{Q}\mathbf{A}^*(\boldsymbol{\theta}_0) + \lambda^2 \mathbf{I}_m \tag{2.2}$$

where $\boldsymbol{\theta}_0 = [\theta_1, \theta_2, \ldots, \theta_n)]^T$, $\mathbf{A}(\boldsymbol{\theta}_0) = [\mathbf{a}(\theta_1), \ldots, \mathbf{a}(\theta_n)]$ is the $(m \times n)$ array manifold matrix, and $\mathbf{Q} = \mathrm{diag}\{q_1, \ldots, q_n\}$ where q_k is the received signal power from $s_k(t)$.

For nonzero source spread, the situation is different. If the distribution of rays from the kth source is Gaussian $N(\theta_k, \sigma_k^2)$, then it can be shown [3] that the array spatial covariance matrix has (μ, ν)th element

$$\mathbf{R}(\mu,\nu) = \left\{ \sum_{k=1}^{n} \frac{q_k}{\sqrt{2\pi}\sigma_k} \int_{-\infty}^{\infty} e^{-\frac{\phi^2}{2\sigma_k^2}} a_\mu(\theta_k+\phi) a_\nu^*(\theta_k+\phi)\, d\phi \right\} + \lambda^2 \delta_{\mu,\nu} \tag{2.3}$$

For a uniform linear array, $a_k(\theta) = e^{j2\pi\Delta(k-1)\sin(\theta)}$, where Δ is the element spacing in wavelengths and θ is the incident angle measured from the broadside of the array. In this case, the integral in (2.3) can be evaluated [3], giving

$$\begin{aligned} \mathbf{R}(\mu,\nu) \;=\; & \left\{ \sum_{k=1}^{n} q_k \left[J_0\left(2\pi\Delta(\mu-\nu)\right) + 2\sum_{l=1}^{\infty} J_{2l}\left(2\pi\Delta(\mu-\nu)\right) e^{-(2l)^2\sigma_k^2} \cos(2l\theta_k) \right.\right. \\ & \left.\left. +2\sum_{l=1}^{\infty} J_{2l-1}\left(2\pi\Delta(\mu-\nu)\right) e^{-(2l-1)^2\sigma_k^2} \sin\left((2l-1)\theta_k\right) \right] \right\} + \lambda^2\delta_{\mu,\nu} \end{aligned} \tag{2.4}$$

where $J_k(x)$ is the kth order modified Bessel function of the first kind.

III. Bias and Variance Analysis of DOA Estimators

A. Small Perturbation Properties of R

We assume the angular spreads σ_i^2 are "small" and derive a first order analysis of the angular spread effect. To this end, we find the Taylor series expansion of $\mathbf{R}$ about the nominal covariance $\mathbf{R_0}$ and retain first order terms in σ_i^2. We find that [7]

$$\mathbf{R} \approx \mathbf{R_0} + \sum_{i=1}^{n} \sigma_i^2 \mathbf{C}_i = \mathbf{R_0} + \mathbf{C} \tag{3.5}$$

where $\mathbf{C}_i = (q_i/2)\cdot[\mathbf{a}(\theta_k)\mathbf{h}^*(\theta_k) + \mathbf{h}(\theta_k)\mathbf{a}^*(\theta_k) + 2\mathbf{d}(\theta_k)\mathbf{d}^*(\theta_k)]$ and where $\mathbf{d}(\theta) = d\mathbf{a}(\theta)/d\theta$ and $\mathbf{h}(\theta) = d^2\mathbf{a}(\theta)/d\theta^2$.

In practice $\mathbf{R}$ is often estimated from N array output samples $\{\mathbf{x}(t)\}_{t=1}^{N}$ by

$$\widehat{\mathbf{R}} = \frac{1}{N}\sum_{t=1}^{N} \mathbf{x}(t)\mathbf{x}^*(t). \tag{3.6}$$

If the elements of $\mathbf{x}(t)$ are given by (2.1), then we find that [7]

$$\widehat{\mathbf{R}} \approx \mathbf{R_0} + \sum_{i=1}^{n} \sigma_i^2 \mathbf{C}_i + \mathbf{M} \tag{3.7}$$

where $\mathbf{M}$ is the random perturbation on $\mathbf{R}$ due to finite sample size N. The finite-sample effects on $\widehat{\mathbf{R}}$ and on the corresponding DOA estimates based on $\widehat{\mathbf{R}}$ are known when $\sigma_k^2 \equiv 0$; see, *e.g.*, [8, 9, 10, 11]. These studies show that $\mathbf{M}$ is a random matrix with mean that is $\mathrm{O}(1/N)$ and standard deviation that is $\mathrm{O}(1/\sqrt{N})$ for large N. We will consider the combined finite sample and source spreading effects. We assume $\sigma_i^2 \approx 1/\sqrt{N}$ and derive expressions for the deviation resulting from both source spread and finite samples. If $\sigma_i^2 \gg 1/N$, then the deviation of $\widehat{\mathbf{R}}$ (and $\widehat{\boldsymbol{\theta}}$) from the nominal value is dominated by $\mathbf{C}$, and finite-sample effects can be neglected; if $\sigma_i^2 \ll 1/N$, then the multipath-induced bias is negligible with respect to finite-sample bias effects.

The DOA estimation algorithms we consider are based on a subspace decomposition of $\widehat{\mathbf{R}}$. We define these subspaces by the decompositions

$$\mathbf{R_0} = \mathbf{S}\mathbf{\Lambda}\mathbf{S}^* + \lambda^2\mathbf{G}\mathbf{G}^* \tag{3.8}$$

$$\widehat{\mathbf{R}} = \widehat{\mathbf{S}}\widehat{\mathbf{\Lambda}}\widehat{\mathbf{S}} + \widehat{\mathbf{G}}\widehat{\mathbf{\Sigma}}\widehat{\mathbf{G}}^* \tag{3.9}$$

where $\mathbf{\Lambda} = \mathrm{diag}\{\lambda_1 \ldots \lambda_n\}$ contains the n largest eigenvalues of $\mathbf{R_0}$, $\mathbf{S}$ is the corresponding matrix of the n associated orthonormal eigenvectors, and $\mathbf{G}$ is the matrix of the remaining $m-n$ orthonormal eigenvectors. We assume $\{\lambda_i\}_{i=1}^n$ are distinct and greater than λ^2. The matrices $\widehat{\mathbf{S}}, \widehat{\mathbf{\Lambda}}, \widehat{\mathbf{G}}$ and $\widehat{\mathbf{\Sigma}}$ are similarly defined. Then as $\sigma_i^2 \to 0$ and $N \to \infty$, we have [5] $\widehat{\mathbf{R}} \to \mathbf{R_0}$, $\widehat{\mathbf{S}} \to \mathbf{S}$, $\widehat{\mathbf{\Lambda}} \to \mathbf{\Lambda}$, $\widehat{\mathbf{\Sigma}} \to \lambda^2\mathbf{I}_{m-n}$, and $\widehat{\mathbf{G}}\widehat{\mathbf{G}}^* \to \mathbf{G}\mathbf{G}^*$. Defining $\mathring{\mathbf{\Lambda}} \triangleq \mathbf{\Lambda} - \lambda^2\mathbf{I}_n$, $(n \times n)$, it readily follows from (3.8) and (3.9) that

$$\mathbf{S}^*\mathbf{R_0}\mathbf{G} = \mathbf{0}, \qquad \widehat{\mathbf{S}}^*\mathbf{G} = \mathring{\mathbf{\Lambda}}^{-1}\mathbf{S}^*\widehat{\mathbf{R}}\mathbf{G}. \tag{3.10}$$

B. The MUSIC Algorithm

The (weighted) MUSIC algorithm computes the DOA estimates $\{\widehat{\theta}_k^M\}_{k=1}^n$ as the n smallest local minima of the function

$$f_M(\theta) = \mathbf{a}^*(\theta)\widehat{\mathbf{G}}\widehat{\mathbf{G}}^*\mathbf{W}\widehat{\mathbf{G}}\widehat{\mathbf{G}}^*\mathbf{a}(\theta) \tag{3.11}$$

where $\mathbf{W}$ is a user-selected non-negative definite Hermitian weighting matrix. A Taylor series expansion of $f_M'(\widehat{\theta}_k)$ about $\widehat{\theta}_k = \theta_k$ for $k = 1, \ldots, n$ gives, to first order [6]

$$\widehat{\theta}_k^M - \theta_k = \frac{-f_M'(\theta_k)}{f_M''(\theta_k)} = \frac{\mathrm{Re}[\mathbf{d}(\theta_k)^*\widehat{\mathbf{G}}\widehat{\mathbf{G}}^*\mathbf{W}\widehat{\mathbf{G}}\widehat{\mathbf{G}}^*\mathbf{a}(\theta_k)]}{\mathbf{d}(\theta_k)^*\widehat{\mathbf{G}}\widehat{\mathbf{G}}^*\mathbf{W}\widehat{\mathbf{G}}\widehat{\mathbf{G}}^*\mathbf{d}(\theta_k)}, \quad k = 1, 2, \ldots, n \tag{3.12}$$

Using (3.5), (3.10), along with properties of orthogonal matrices, we can show that, to first order [7]

$$\widehat{\theta}_k^M - \theta_k = \frac{-\,\mathrm{Re}\left\{\mathbf{d}_k^*\mathbf{G}\mathbf{G}^*\mathbf{W}\mathbf{G}\mathbf{G}^*\left[\sum_{i=1}^n \sigma_i^2\mathbf{C}_i + \mathbf{M}\right]\mathbf{S}\mathring{\mathbf{\Lambda}}^{-1}\mathbf{G}\mathbf{S}^*\mathbf{a}_k\right\}}{\mathbf{d}_k^*\mathbf{G}\mathbf{G}^*\mathbf{W}\mathbf{G}\mathbf{G}^*\mathbf{d}_k} \tag{3.13}$$

$$\triangleq \sum_{i=1}^n \sigma_i^2 b_{ik}^M + \tilde{\theta}_k^M, \qquad k = 1, \ldots, n. \tag{3.14}$$

Each b_{ik}^M term corresponds to the bias of the kth DOA estimate due to the angular spread of the ith source. The $\tilde{\theta}_k^M$ term is a random variable whose mean is $\mathrm{O}(1/N)$ and whose standard deviation is $\mathrm{O}(1/\sqrt{N})$. For $\sigma_i \equiv 0$, equation (3.13) reduces to the large-sample expression for the MUSIC estimation error derived in [8] for the nominal signal model.

C. The ESPRIT Algorithm

The ESPRIT algorithm is derived under the assumption that the array has a shift invariant structure. That is, the array elements can be partitioned into two subsets, which are identical except for a translational shift of δ wavelengths. Thus, the array

manifold matrix $\mathbf{A}(\boldsymbol{\theta})$ satisfies $[0 \quad \mathbf{I}_{\bar{m}}]\mathbf{A}(\boldsymbol{\theta}) = [\mathbf{I}_{\bar{m}} \quad 0]\mathbf{A}(\boldsymbol{\theta})\Psi$, where Ψ is a diagonal matrix with diagonal elements $\{e^{i\omega_k}\}_{k=1}^{\bar{m}}$. If we define the $(m \times n)$ matrices $\widehat{\mathbf{S}}_1 = [\mathbf{I}_{\bar{m}} \quad 0]\widehat{\mathbf{S}}$ and $\widehat{\mathbf{S}}_2 = [0 \quad \mathbf{I}_{\bar{m}}]\widehat{\mathbf{S}}$, and the $(n \times n)$ matrix $\hat{\phi} = (\widehat{\mathbf{S}}_1^*\widehat{\mathbf{S}}_1)^{-1}\widehat{\mathbf{S}}_1^*\widehat{\mathbf{S}}_2$, then the ESPRIT direction of arrival estimates are given by

$$\widehat{\theta}_k^E = \sin^{-1}\left(\frac{\arg\hat{\rho}_k}{2\pi\delta}\right), \quad k = 1, \ldots, n, \tag{3.15}$$

where $\{\hat{\rho}_k\}_{k=1}^n$ are the eigenvalues of $\hat{\phi}$. Using an expression for $\hat{\phi}$ developed in [5] along with (3.15) (see [7] for details), we can show that to first order

$$\widehat{\theta}_k^E - \theta_k = \frac{1}{2\pi\delta\cos\theta_k}\,\mathrm{Im}\left\{\frac{1}{\rho_k}\mu_k^*\left[\sum_{i=1}^n \sigma_i^2\mathbf{C}_i + \mathbf{M}\right]\mathbf{S}\mathring{\mathbf{\Lambda}}^{-1}\beta_k\right\} \tag{3.16}$$

$$\triangleq \sum_{i=1}^n \sigma_i^2 b_{ik}^E + \tilde{\theta}_k^E, \tag{3.17}$$

where $\mu_k^* = \gamma_k^*(\mathbf{S}_1^*\mathbf{S}_1)^{-1}\mathbf{S}_1^*\{[0 \quad \mathbf{I}_{\bar{m}}] - \rho_k[\mathbf{I}_{\bar{m}} \quad 0]\}$, ρ_k, γ_k, β_k are the eigenvalues and the associated left and right eigenvectors (normalized so the $\gamma_k^*\beta_k = 1$) of the matrix $\phi = (\mathbf{S}_1^*\mathbf{S}_1)^{-1}\mathbf{S}_1^*\mathbf{S}_2$, with $\mathbf{S}_1 = [\mathbf{I}_{\bar{m}} \quad 0]\mathbf{S}$ and $\mathbf{S}_2 = [0 \quad \mathbf{I}_{\bar{m}}]\mathbf{S}$. In (3.17), $\tilde{\theta}_k^E$ is the expression for the first order perturbation of the ESPRIT method without source spread [12, 13]. Once again, the DOA bias is dominated by the spatial spread, and the variance is to first order the nominal ESPRIT variance.

D. The WSF Algorithm

The WSF algorithm [10] involves the maximization of the cost function:

$$\widehat{\boldsymbol{\theta}}^W = \arg\max \mathbf{V}(\boldsymbol{\theta}) \tag{3.18}$$

where $\widehat{\boldsymbol{\theta}}^W = [\widehat{\theta}_1^W, \ldots, \widehat{\theta}_n^W]^T$ is the vector of DOA estimates from WSF and where

$$\mathbf{V}(\boldsymbol{\theta}) = \mathrm{tr}\left[\mathbf{A}(\boldsymbol{\theta})\left[\mathbf{A}^*(\boldsymbol{\theta})\mathbf{A}(\boldsymbol{\theta})\right]^{-1}\mathbf{A}^*(\boldsymbol{\theta})\widehat{\mathbf{S}}\mathbf{W}\widehat{\mathbf{S}}^*\right] \tag{3.19}$$

The matrix $\mathbf{W}$ is a user-selected weighting matrix. The optimal weight $\mathbf{W}_{\mathrm{opt}} \triangleq \mathring{\mathbf{\Lambda}}^2\mathbf{\Lambda}^{-1}$, or a consistent estimate of it, is often used because the resulting DOA estimates have asymptotically minimum variance over all such weighting matrices [10, 11].

The deviation in the DOA estimates can be found from a Taylor series expansion of $\mathbf{V}'(\widehat{\boldsymbol{\theta}})$ about the point $\boldsymbol{\theta}_0$; this yields [10, 11]

$$\widehat{\boldsymbol{\theta}}^W - \boldsymbol{\theta}_0 \approx -[\mathbf{V}''(\boldsymbol{\theta}_0)]^{-1}\mathbf{V}'(\boldsymbol{\theta}_0) \tag{3.20}$$

where $\mathbf{V}'(\boldsymbol{\theta}_0)$ and $\mathbf{V}''(\boldsymbol{\theta}_0)$ are the gradient vector and Hessian matrix of $\mathbf{V}(\boldsymbol{\theta})$. Using the results in [10, 11], along with (3.7) and (3.10), we obtain to first order that

$$\mathbf{V}_k'(\boldsymbol{\theta}_0) = 2\mathrm{Re}\left\{\mathbf{e}_k^T\mathbf{A}^\dagger\mathbf{S}\mathbf{W}\mathring{\mathbf{\Lambda}}^{-1}\mathbf{S}^*\left[\sum_{i=1}^n \sigma_i^2\mathbf{C}_i + \mathbf{M}\right]\mathbf{G}\mathbf{G}^*\mathbf{d}(\theta_k)\right\} \tag{3.21}$$

$$\mathbf{V}''(\boldsymbol{\theta}_0) = -2\mathrm{Re}[(\mathbf{A}^\dagger\mathbf{S}\mathbf{W}\mathbf{S}^*\mathbf{A}^\dagger)^* \odot \mathbf{D}^*\mathbf{G}\mathbf{G}^*\mathbf{D}] \tag{3.22}$$

where $\mathbf{V}'_k(\boldsymbol{\theta}_0)$ is the kth element of $\mathbf{V}'(\boldsymbol{\theta}_0)$, $\mathbf{e}_k$ is the kth unit vector, $\mathbf{A} = \mathbf{A}(\boldsymbol{\theta}_0)$, $\mathbf{A}^\dagger = (\mathbf{A}^*\mathbf{A})^{-1}\mathbf{A}^*$, and $\mathbf{D} = [\mathbf{d}(\theta_1)\ldots\mathbf{d}(\theta_n)]$. Inserting (3.22) and (3.21) into (3.20) gives the final result for the deviation; to first order it can be expressed as

$$\widehat{\boldsymbol{\theta}}^W - \boldsymbol{\theta}_0 \triangleq \sum_{i=1}^{n} \sigma_i^2 \mathbf{b}_i^W + \tilde{\boldsymbol{\theta}}^W \tag{3.23}$$

Once again, to first order the bias of $\widehat{\boldsymbol{\theta}}^W$ is dominated by the source spread, and the variance of $\widehat{\boldsymbol{\theta}}^W$ is the same as the nominal WSF variance as derived in [10, 11].

E. Variance Considerations

The variance of the DOA estimates from MUSIC, ESPRIT, and WSF when source spread is present, are to first order equal to the "nominal" variances when there is no source spreading. It can be shown from equation (3.14), (3.17), or (3.23) that the variance of the DOA estimates increases linearly with σ_k^2 for small σ_k [7]. The slope of this variance increase is given by $E\{\tilde{\theta}\}$. The term $E\{\tilde{\theta}\}$ is known to be $\mathrm{O}(1/N)$ for the three methods we consider. For MUSIC, an analytic expression for $E\{\tilde{\theta}_k^M\}$ is derived in [14]; no similar expressions seems to be available for ESPRIT and WSF.

F. Uniform Linear Array and Single Source

For a uniform linear array and a single source, it can be shown from equations (3.13), (3.16), and (3.23) that the first order bias term of the DOA estimate is given by

$$\theta_b^M = \theta_b^E = \theta_b^W = \frac{-\sigma_1^2}{2}\tan\theta_1. \tag{3.24}$$

It is remarkable not only that the three bias terms are equal, but that they are also independent of the array size m, the signal power q_1, and the noise power λ^2.

The bias term in equation (3.24) can also be found by purely geometrical arguments. For a ULA, the phase shift between adjacent elements that results from a signal arriving at angle θ is given by $\omega = f(\theta) = 2\pi\Delta\sin\theta$. If θ is a random variable with small, then a nonzero bias in ω results from the asymmetry of f around θ. This bias, transformed back from ω to θ is exactly the bias expression in equation (3.24). This argument suggests that the bias of the DOA estimates may result from array geometry in some cases.

IV. Numerical Exmples

We present numerical examples that illustrate the DOA bias and variance due to source spread and finite samples. We consider a ULA with half wavelength spacing of the elements. We show results for the MUSIC algorithm, but the ESPRIT and WSF results are nearly identical to those presented. The "true bias" results are obtained by applying the DOA algorithms to $\mathbf{R}$ as given in equation (2.4), and the "first order bias" results are generated from equations (3.13), (3.16), and (3.23).

Figure 1 compares the (negative of the) actual DOA bias to that predicted by the first order theory for a 5-element ULA and for a single source with angular spread standard deviation of $\sigma_1 = 5^\circ$. Figure 1b shows the ratio of the first order bias to the total bias for varying signal spread standard deviations. We see that the first order theory predicts the bias well for $\sigma_1 \leq 3^\circ$. The large relative errors near $\theta = 0^\circ$ occur where the absolute error is quite small, as can be seen from Figure 1a. We note that for mobile telecommunications, angular spreads of $\sigma_\theta \approx 1 - 4^\circ$ have been reported [3]; thus, the first order theory appears to be useful in this application.

Figure 2 compares the first order bias to the actual bias for a single source and $N = \infty$, as a function of source spread σ_1 and array size m. Two cases are shown corresponding to arrival angles of -20° and -75°; note the different bias scales for the two plots. The deviation of first order theory from true bias can be shown to depend on the product $m\Delta \cdot \sigma_1$, because this controls the total phase deviation across the entire array [7].

Figure 3 compares the infinite sample true and first order bias to finite sample estimates. Again the array is a 5-element ULA, and a single source arrives at a nominal angle of -75°. The error bars show the 1-standard deviation angle estimation errors for 200 Monte-Carlo simulation trials. We see the predicted linear trend in bias for increasing σ_1^2. We also see an approximately linear increase in DOA variance for increasing σ_1^2.

Figure 4 compares the true biases (for $N = \infty$) and first-order bias predictions for a 10-element ULA with two equal power sources. One source is fixed at $\theta = 20^\circ$ and the other source direction is varied. The source spread standard deviations are both set to 3°. When the θ_2 is near 20°, the bias becomes very large; in this region, the MUSIC algorithm fails to resolve the two sources, even for $N = \infty$. We also see an oscillatory behavior in the bias, which is similar to "bias leakage" in DFT-based spectral analysis. We have found similar oscillatory behavior in the MUSIC loss function. As the signal powers of the two sources differ, the minimum corresponding to the weaker source becomes "lost" in these ripples of the loss function, and the MUSIC algorithm fails to detect the weaker source; similar detection failures were found for ESPRIT and WSF. Thus, for applications with large differences in source signal powers and multipath, these DOA estimators may not apply unless some modifications are made to address this problem.

V. Conclusions

We have analyzed the effect that angular spread of signal sources have on the direction of arrival estimates of three direction-of-arrival estimation algorithms: MUSIC, ESPRIT, and WSF. We derived analytical expressions for the bias of the DOA estimates under the assumption that the signal spread was small. To first order, the DOA bias depends linearly on the variance of the angular spread. The variance of the DOA estimates is the "nominal" variance for the case when there is no source spread; this variance also increases linearly with source spread variance.

We compared our first order analysis to the true bias, and found good agreement for

practical source spread values. For two or more sources, all source signals contribute to the bias of each DOA estimate; this bias contribution can be significant, even if the sources are well-separated. For a uniform linear array and a single source, all three methods have the same DOA estimate bias to first order. This first-order bias is independent of signal or noise power and of array size. An identical first-order bias expression was obtained from an analysis that relied only on the array geometry.

For most cases we considered, the bias induced by source spread was never very large. The standard deviation from the DOA estimates due to finite sample estimation of the array covariance matrix often dominated the bias. Thus, the bias analysis predicts, and the simulations verify, that the use of MUSIC, ESPRIT, and WSF result in DOA estimates that are only slightly affected by source spreading for most signal scenarios. On the other hand, source spread resulted in an oscillatory cost function for MUSIC and the extra local minima resulted in failure to detect weak sources; similar detection failures were found for ESPRIT and WSF. These extra minima could cause the algorithm to fail to locate a weak source signal.

VI. References

[1] J. Salz and J. H. Winters, "Effect of fading correlation on adaptive arrays in digital wireless communication," in *Proceedings of the International Conference on Communications*, (Geneva), pp. 1768–1774, May 1993.

[2] P. Zetterberg and B. Ottersten, "The spectrum efficiency of a basestation antenna array system for spatially selective transmission," in *Proceedings of the 43rd IEEE Vehicular Technology Conference*, (Stockholm, Sweden), pp. 1517–1521, 1994.

[3] T. Trump and B. Ottersten, "Estimation of nominal direction of arrival and angular spread using an array of sensors," Technical Report IR-S3-SB-9424, Royal Institute of Technology, Stockholm, Sweden, October 1994. (also submitted to *Signal Processing*).

[4] M. Viberg and A. L. Swindlehurst, "Analysis of the combined effects of finite samples and model errors on array processing performance," *IEEE Transactions on Signal Processing*, vol. 42, pp. 3073–3083, November 1994.

[5] A. Kangas, P. Stoica, and T. Söderström, "Finite sample and modelling error effects on ESPRIT and MUSIC direction estimators," *IEE Proceedings - Radar, Sonar and Navigation*, vol. 141, pp. 249–255, October 1994.

[6] A. Kangas, P. Stoica, and T. Söderström, "Large-sample analysis of MUSIC and Min-Norm direction estimators in the presence of model errors," *Circuits, Systems, and Signal Processing*, 1995. (to appear).

[7] R. Moses, T. Söderström, and J. Sorelius, "Effects of multipath-induced angular spread on direction of arrival estimators in array signal processing," Technical

Report UPTEC 95005R, Department of Technology, Uppsala University, February 1995.

[8] P. Stoica and A. Nehorai, "MUSIC, Maximum Likelihood, and Cramér-Rao Bound," *IEEE Transactions on Acoustics, Speech, and Signal Processing*, vol. ASSP–37, pp. 720–741, May 1989.

[9] P. Stoica and A. Nehorai, "MUSIC, maximum likelihood, and Cramér-Rao bound: further results and comparisons," *IEEE Transactions on Acoustics, Speech, and Signal Processing*, vol. ASSP-38, pp. 2140–2150, December 1990.

[10] M. Viberg and B. Ottersten, "Sensor array processing based on subspace fitting," *IEEE Transactions on Signal Processing*, vol. 39, pp. 1110–1121, May 1991.

[11] B. Ottersten, M. Viberg, P. Stoica, and A. Nehorai, "Exact and large sample maximum likelihood techniques for parameter estimation and detection in array processing," in *Radar Array Processing* (S. Haykin, J.Litva, and T. J. Shephard, eds.), pp. 99–151, New York: Springer Verlag, 1993.

[12] R. Roy and T. Kailath, "ESPRIT—estimation of signal parameters via rotational invariance techniques," *IEEE Transactions on Acoustics, Speech, and Signal Processing*, vol. ASSP-37, pp. 984–995, July 1989.

[13] P. Stoica and A. Nehorai, "Performance comparison of subspace rotation and MUSIC methods for direction estimation," *IEEE Transactions on Signal Processing*, vol. 39, pp. 446–453, February 1991.

[14] X.-L. Xu and K. M. Buckley, "Bias analysis of the MUSIC location estimator," *IEEE Transactions on Signal Processing*, vol. 40, pp. 2559–2569, 1992.

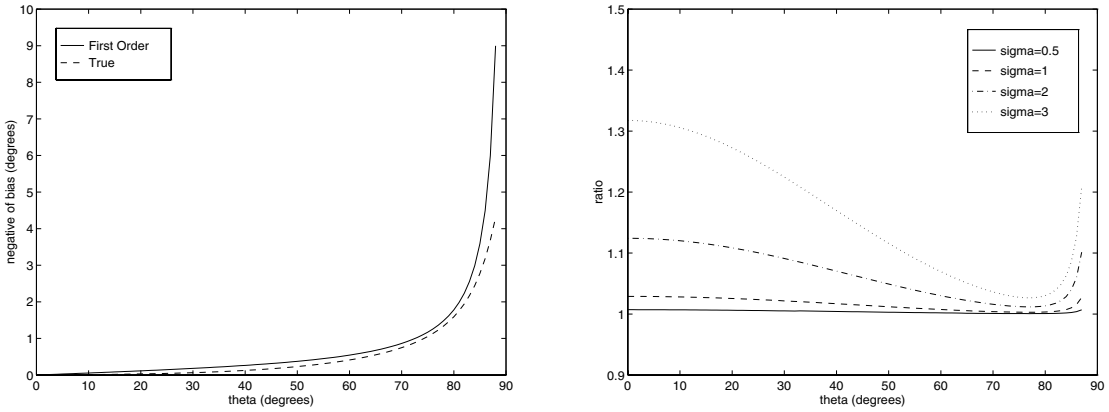

(a) Negative of Bias (b) Ratio of first order to true bias

Figure 1: Comparison of true bias and first order bias for MUSIC, using a single source with spread $\sigma_1 = 5^\circ$

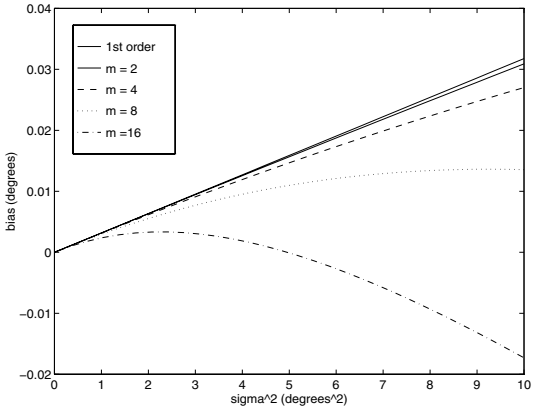

(a) $\theta_1 = -20°$

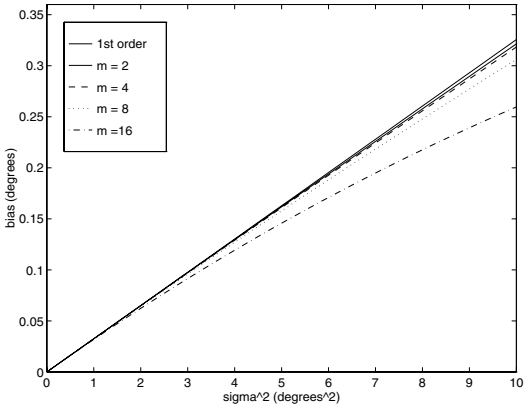

(b) $\theta_1 = -75°$.

Figure 2: Effect of number of array elements on MUSIC bias, for a single source.

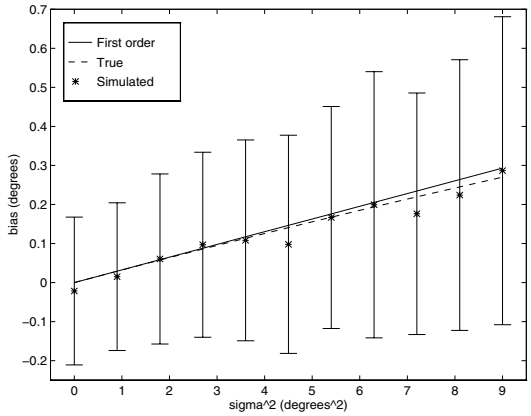

(a) $N = 100$ data samples

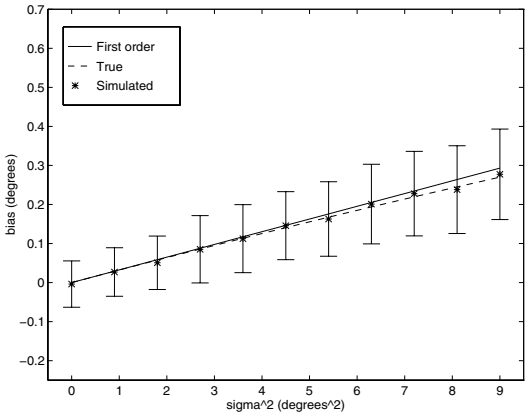

(b) $N = 1000$ data samples

Figure 3: Comparison of infinite sample and finite sample biases for MUSIC for a 5-element ULA with a single source at $\theta_1 = -75°$. Error bars are sample 1 standard deviation errors from 200 Monte-Carlo simulations.

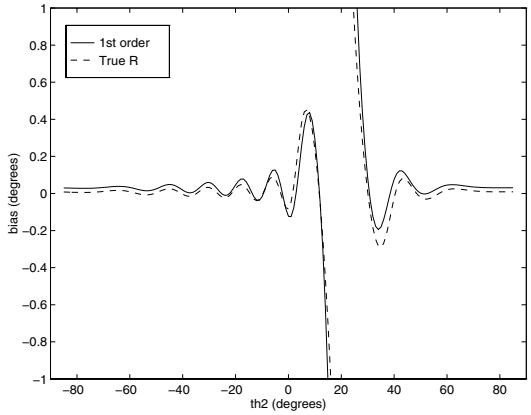

(a)bias for $\theta_1 = 20°$

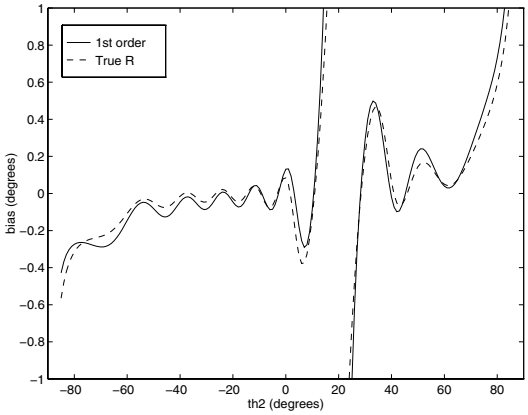

(b) bias for θ_2

Figure 4: True and first order bias for two sources, as a function of θ_2.